

Supporting Information for

Intriguing electronic and optical prospects of FCC bimetallic two-dimensional heterostructures: epsilon near-zero behaviour in UV-vis range

Tuhin Kumar Maji¹, Kumar Vaibhav², Ranjit Hawaldar³, K. V. Adarsh⁴, Samir Kumar Pal¹ and Debjani Karmakar^{5,*}

¹*Department of Chemical Biological and Macromolecular Sciences, S.N. Bose National Centre for Basics Sciences, Salt Lake, Sector 3, Kolkata 700106, India*

²*Computer Division, Bhabha Atomic Research Centre, Trombay 400085, India*

³*Centre for Materials for Electronics Technology, Off Pashan Road, Panchwati, Pune-411008, India*

⁴*Department of Physics, Indian Institute of Science Education and Research, Bhopal 462066, India*

⁵*Technical Physics Division, Bhabha Atomic Research Centre, Trombay 400085, India*

*Corresponding author:

Debjani Karmakar: debjan@barc.gov.in

METHODOLOGY:

Optical Property Calculation

A. TDDFT Formulation

TDDFT aims at mapping the time-dependent Schrödinger equation onto an effective one-electron problem, where time dependence is incorporated in the approximation of the exchange-correlation kernel (xck) from the explicit time dependence of the exchange-correlation potential and electron-density as:

$$f_{xc}(r, r', t - t') = \frac{\partial v_{xc}(r, t)}{\partial \rho(r', t')} \quad (1)$$

Calculation of optical absorption involves many-body perturbative approach of solution of Bethe Salpeter Equation (BSE) using the one-body Green's function. In BSE, the dielectric function can be written in terms of the xck as [1] :

$$\epsilon_{GG}^{-1}(q, \omega) = \delta_{GG} + v_{GG}(q) \chi'(q, \omega), \quad (2)$$

where $v(q)$ is the bare Coulomb potential and χ is the full response function, which is related to the response function χ^0 of the non-interacting Kohn-Sham system as:

$$\chi'(q, \omega) = \frac{v_{GG}(q) \chi_{GG}^0(q, \omega)}{1 - [v_{GG}(q) + f_{xc}(q, \omega)] \chi_{GG}^0(q, \omega)} \quad (3)$$

The frequency independent approximation for the xck, known as the Bootstrap kernel, is computationally less exorbitant than a rigorous solution of the BSE:

$$f_{xc}^{TDDFT}(q, \omega) = \frac{\epsilon^{-1}(q, \omega = 0)}{\chi_{GG}^0(q, \omega = 0)} \quad (4)$$

The coupled equations (2), (3) and (4) are solved by initially setting $f_{xc}^{TDDFT} = 0$ and then calculating $\chi'(q, \omega)$ and thus $\epsilon_{GG}^{-1}(q, \omega)$. This value is then utilized in equation (6) to find out the new f_{xc}^{TDDFT} . This procedure is repeated until self-consistency is obtained at $\omega = 0$.

The long-range component of exchange-correlation kernel is frequency independent having the form $-\alpha^{\text{static}} / q^2$. More detailed and accurate formulation involves introducing frequency dependence. The long-range contribution kernel (LRC) assimilates the frequency dependence in the following form into the dynamical exchange:

$$f_{xc}^{\text{dyn}}(q, \omega) = -\frac{1}{q^2}(\alpha + \beta\omega^2) \quad (5)$$

This improvement of dynamical kernel has improved the calculations to obtain important information about the exciton and charged excitons[2].

B. Interband and intraband contribution to the dielectric response function

The real and imaginary parts of the interband dielectric response function in tensor form are computed as[3]:

$$\begin{aligned} \epsilon_{\alpha\beta}^{(1)}(\hat{q}, \omega) &= 1 + \frac{4\pi e^2}{V} \lim_{q \rightarrow 0} \frac{1}{q^2} \sum_{nmk} 2f_{nk} \langle u_{mk+e_{\alpha q}} | u_{nk} \rangle \langle u_{nk} | u_{mk+e_{\beta q}} \rangle \times \left(\frac{1}{\epsilon_{mk} - \epsilon_{nk} - \omega} + \frac{1}{\epsilon_{mk} - \epsilon_{nk} + \omega} \right) \end{aligned} \quad (6)$$

and

$$\begin{aligned} \epsilon_{\alpha\beta}^{(2)}(\hat{q}, \omega) &= \frac{4\pi^2 e^2}{V} \lim_{q \rightarrow 0} \frac{1}{q^2} \sum_{nmk} 2f_{nk} \langle u_{mk+e_{\alpha q}} | u_{nk} \rangle \langle u_{nk} | u_{mk+e_{\beta q}} \rangle \times (\delta(\epsilon_{mk} - \epsilon_{nk} - \omega) - \delta(\epsilon_{mk} - \epsilon_{nk} + \omega)) \end{aligned} \quad (7)$$

For semiconductors and insulators, only interband transitions are important ($n \neq m$). For metals, due to the occurrence of partially occupied bands, transitions within a band, often referred to as intra-band transitions are also important. The real part of intra-band dielectric function, dependent only on frequency of the incident light and the energy dispersion, can be written as:

$$\epsilon_{\alpha\beta}^{1 \text{ intra}} = -\frac{\bar{\omega}_{\alpha\beta}^2}{\omega^2} \quad (8)$$

where $\bar{\omega}_{\alpha\beta}$ is the material specific property, referred to as the plasma frequency tensor, represented as:

$$\bar{\omega}_{\alpha\beta}^2 = \frac{4\pi e^2}{V} \sum_{nk} 2f_{nk} \frac{\partial^2 \epsilon_{nk}}{\partial k_\alpha \partial k_\beta} \quad (9)$$

The imaginary part is obtained from the Kramers-Kronig transformation:

$$\epsilon_{\alpha\beta}^2 = -\pi \bar{\omega}_{\alpha\alpha}^2 \frac{\partial \delta(\omega)}{\partial \omega} \quad (10)$$

After introducing the relaxation-time τ under semiclassical approximation, the real and imaginary part of the intraband dielectric function can be written as:

$$\epsilon^1(\omega) = 1 - \frac{\bar{\omega}^2 \tau^2}{1 + \omega^2 \tau^2} \quad (11)$$

$$\epsilon^2(\omega) = \frac{\bar{\omega}^2 \tau}{\omega(1 + \omega^2 \tau^2)} \quad (12)$$

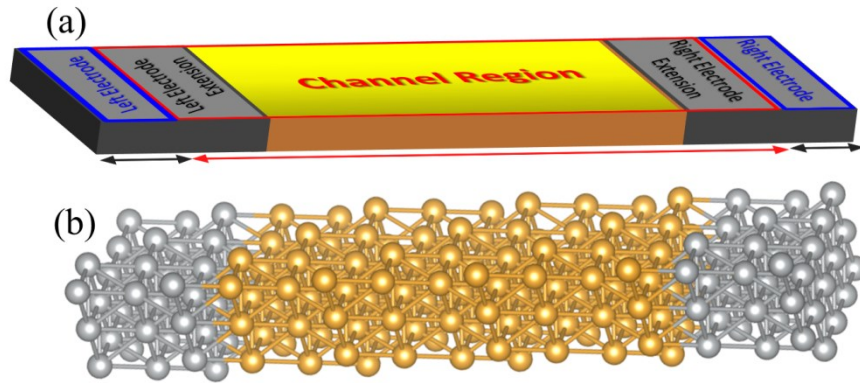
Therefore, for metals, the intra-band dielectric function has a near-zero frequency negative and positive divergence respectively for real and imaginary parts, which constitutes the ‘‘Drude-like’’ terms.

Transmission coefficients calculation

Γ -point centred interpolated transmission coefficients at zero bias perpendicular to the transport axis within the irreducible Brillouin zone (IBZ) are obtained for both the device geometries by using:

$$T^\parallel(E) = Tr[\Gamma_L^\parallel(E) g_\parallel(E) \Gamma_R^\parallel(E) g_\parallel^\dagger(E)] \quad (13)$$

where, g_\parallel is the retarded Green’s function, $\Gamma_{L/R}$ is the level broadening with respect to the corresponding self-energies of the electrodes. This function, while integrated over the k -point mesh in the IBZ, results the transmission coefficient.



Scheme S1 (a) A model device configuration having two electrodes, electrode extension and a central region, (b) model Au-channel Ag contact system.

Table S1: Bader Charge table of different systems

System	Total Charge (ideal)	Total Charge Bader	Ag Part		Au Part	
			Ideal Charge	Bader Charge	Ideal Charge	Bader Charge
Au/Ag-111 Embedded	378	383.46	141	168.78	237	214.68
	20439	20001.45	2585	2534.65	17854	17466.8
Ag-doped Au	3536	3607.74	376	371.54	3160	3236.20

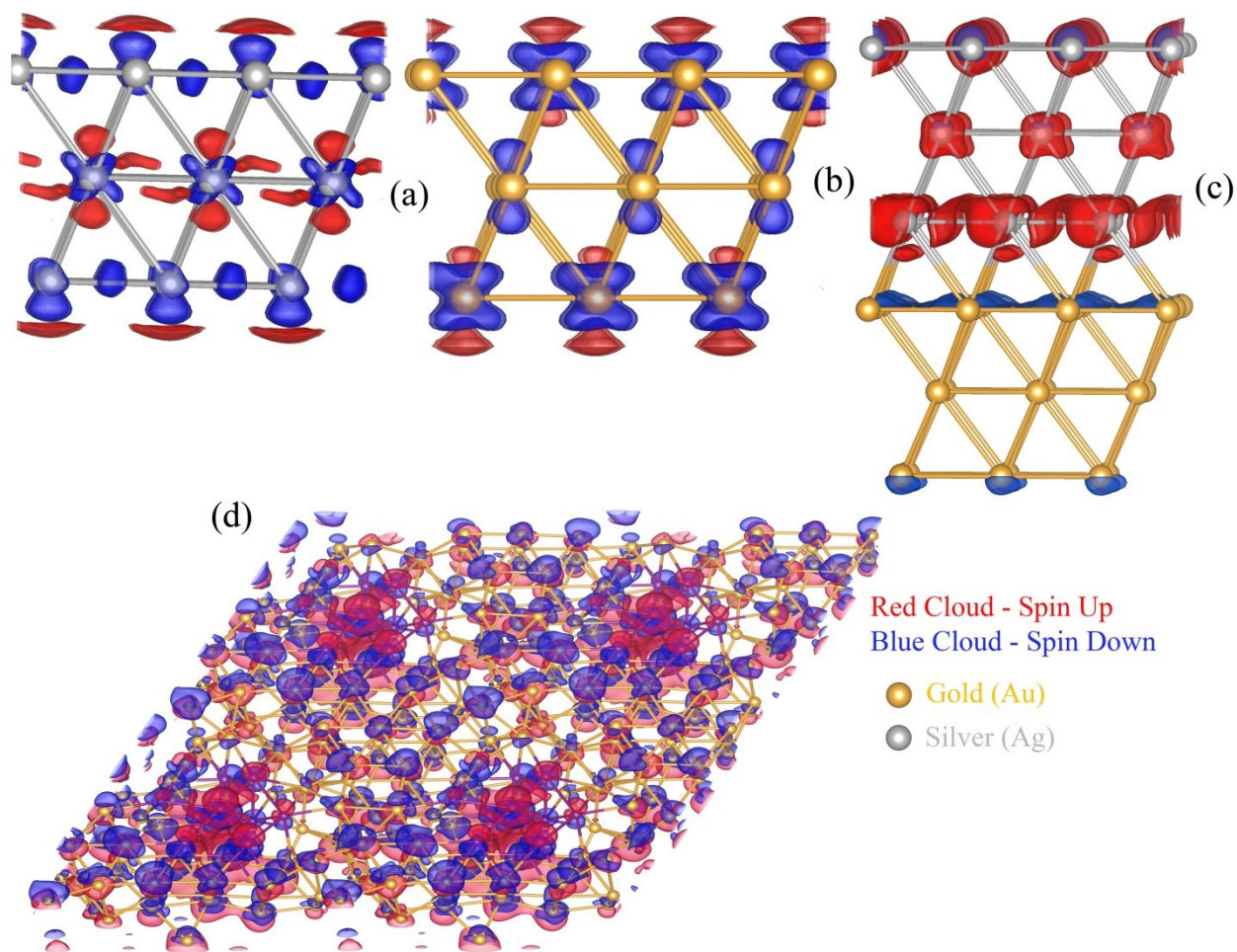


Figure S1: Converged spin density plot for a) Ag111, b) Au111, c) Au/Au-111 and d) Embedded system.

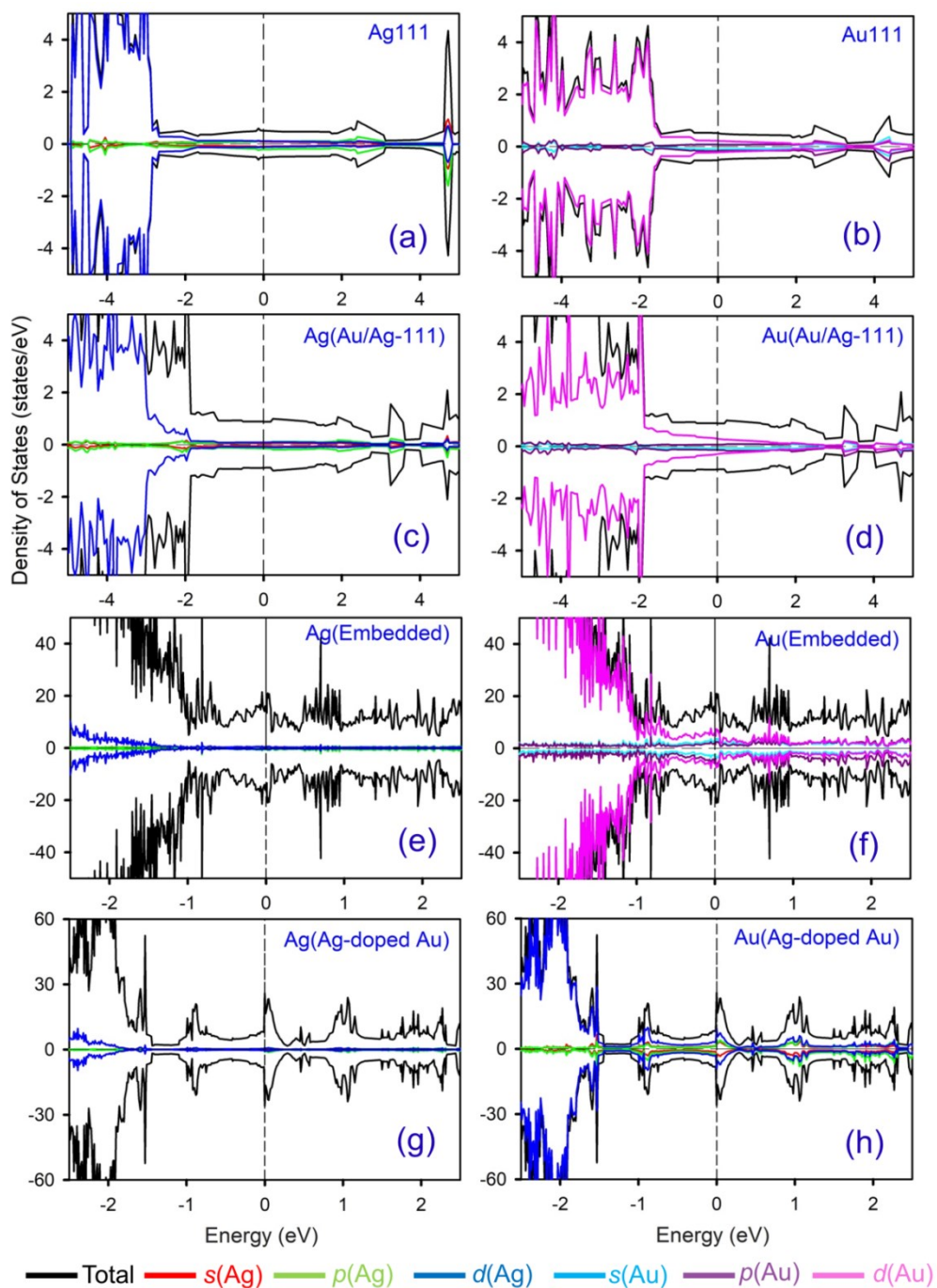


Figure S2: Orbital Projected Density of States for a) Ag111, b) Au111, c) contribution of Ag in Au/Ag-111, d) contribution of Au in Au/Ag-111, e) contribution of Ag in embedded, f) contribution of Au in embedded, g) contribution of Ag in Ag-doped Au and h) contribution of Au in Ag-doped Au

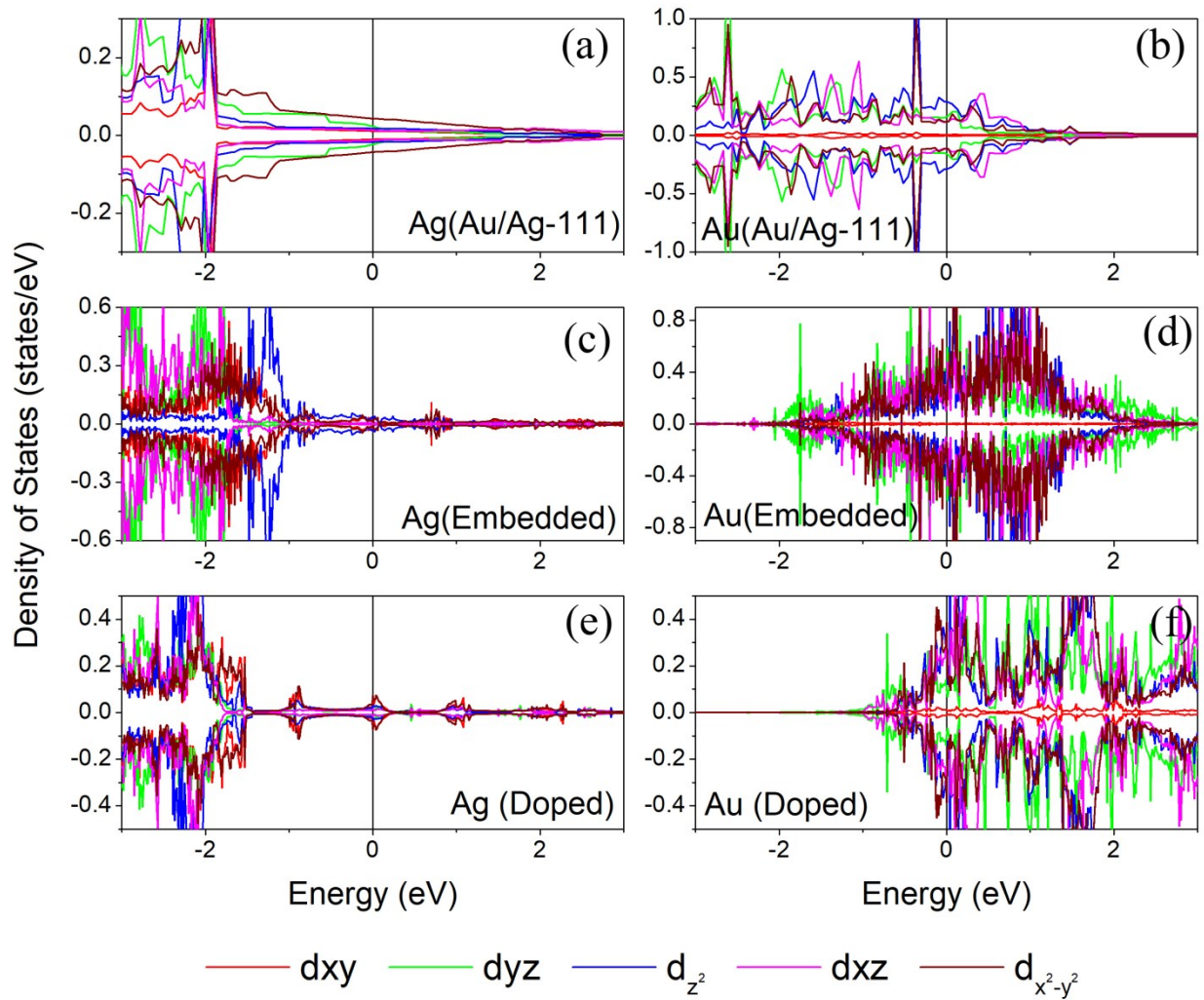


Figure S3: *d*-orbital Projected Density of States for a) contribution of Ag in Au/Ag-111, b) contribution of Au in Au/Ag-111, c) contribution of Ag and d) contribution of Au in embedded system, e) contribution of Ag and f) contribution of Au in doped system.

Pd-Pt system

For this combination, we have created large-area interfaces created from Pt[111] and Pd[111]. The doped nanostructure was formed by doping Pt[111] matrix centrally with some Pd atoms. Both of these systems are having interesting optical properties. The epsilon-near-zero property, energy-zero divergence and the negative value of real part of epsilon is present as can be seen from Fig S5. Partially filled *d*-bands of both Pt and Pd generate flat-bands near Fermi-level.

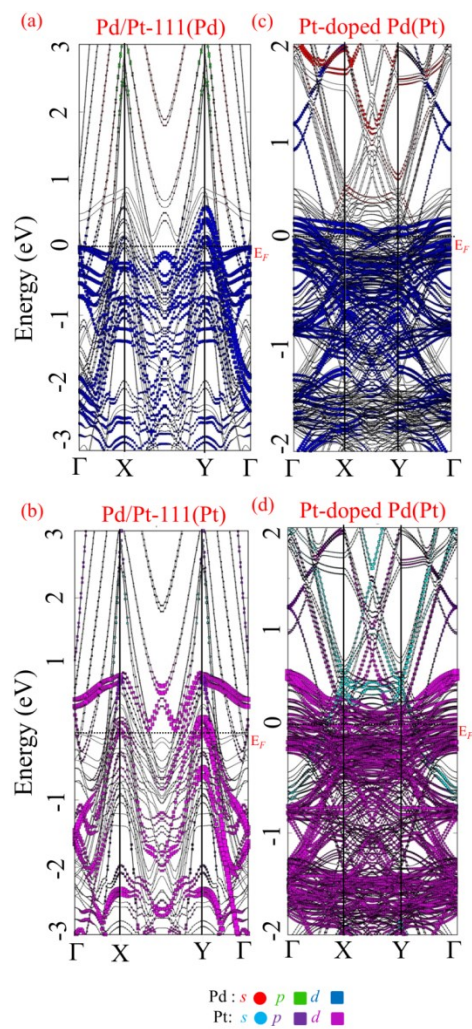


Figure S4: The orbital projected fatbands for orbital components of a) Pd in Pt/Pd-111 system, b) Pt in Pt/Pd-111 system, c) Pd in Pd-doped Pt system and d) Pt in Pd-doped Pt system.

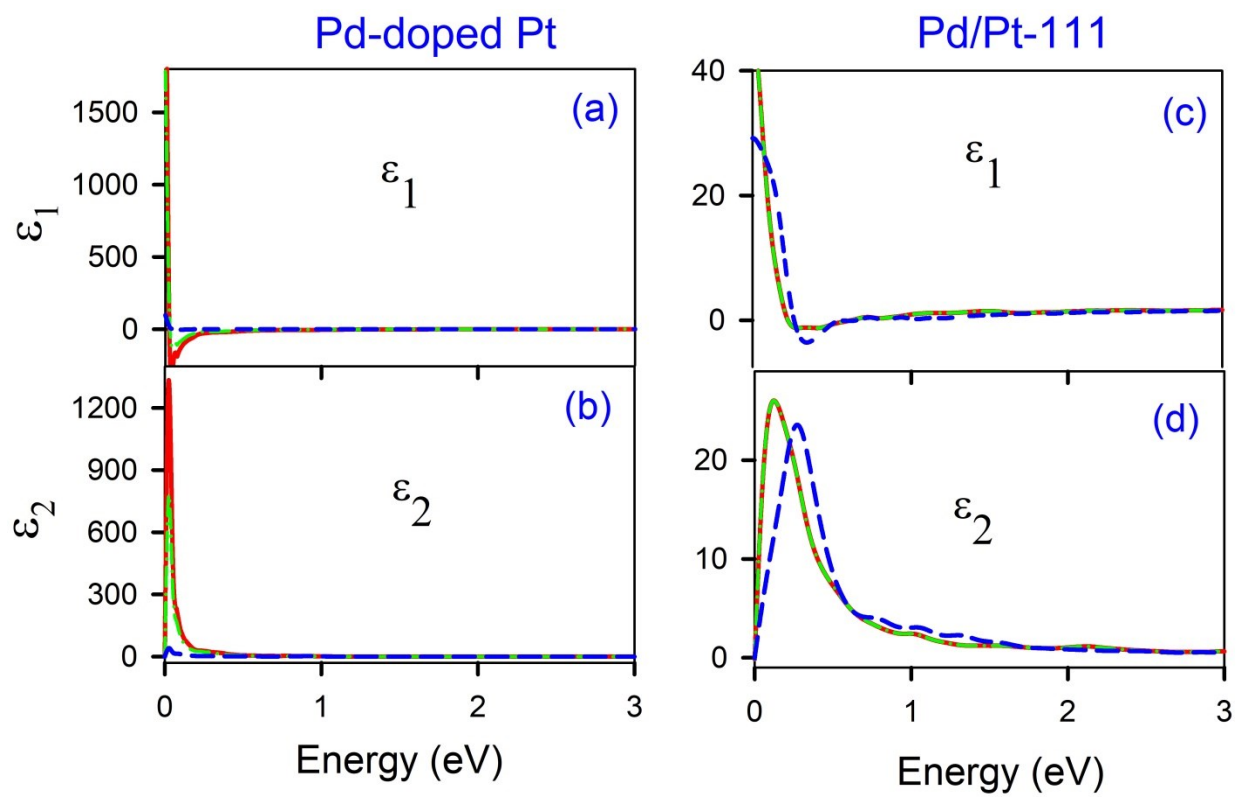


Figure S5: Real and Imaginary part of dielectric constant of Pd-doped and Pd/Pt-111 system.

References

- [1] M. Dadsetani and A. R. Omid, RSC Advances **5**, 90559 (2015).
- [2] S. Botti, A. Fourreau, F. Nguyen, Y.-O. Renault, F. Sottile and L. Reining, Physical Review B **72**, 125203 (2005).
- [3] J. Harl, The Linear Response Function in Density Functional Theory (Dissertation), University of Vienna, 2008.